Title
Intussusceptive Angiogenesis in Human Metastatic Malignant Melanoma

Journal
American Journal Of Pathology, 191(11)

ISSN
0002-9440

Authors
Pandita, Ankur
Ekstrand, Matias
Bjursten, Sara
et al.

Publication Date
2021-11-01

DOI
10.1016/j.ajpath.2021.07.009

Peer reviewed

The American Journal of Pathology, Vol. 191, No. 11, November 2021

ELSEVIER

The American Journal of PATHOLOGY

ajp.amjpathol.org

TUMORIGENESIS AND NEOPLASTIC PROGRESSION

Intussusceptive Angiogenesis in Human Metastatic Malignant Melanoma

Ankur Pandita,*†‡ Matias Ekstrand,* Sara Bjursten,†‡ Zhiyuan Zhao,*†‡ Per Fogelstrand,* Kristell Le Gal,§ Lars Ny,†‡§ Martin O. Bergo,¶ Joakim Karlsson,§ Jonas A. Nilsson,§ Levent M. Akyürek,‖ Malin C. Levin,* Jan Borén,* Andrew J. Ewald,**†† Keith E. Mostov,‡‡ and Max Levin*†‡

From the Wallenberg Laboratory for Cardiovascular Research, Department of Molecular and Clinical Medicine, and the Department of Oncology,† Institute of Clinical Sciences, Sahlgrenska Academy, and the Sahlgrenska Center for Cancer Research,§ University of Gothenburg, Gothenburg, Sweden; the Departments of Oncology‡ and Pathology,‖ Sahlgrenska University Hospital, Gothenburg, Sweden; the Department of Biosciences and Nutrition,¶ Karolinska Institutet, Stockholm, Sweden; the Department of Cell Biology,** Johns Hopkins University, Baltimore, Maryland; the Department of Oncology,†† Cancer Invasion and Metastasis Program, Sidney Kimmel Comprehensive Cancer Center, Johns Hopkins University, Baltimore, Maryland; and the Departments of Anatomy and Biochemistry/Biophysics,‡‡ University of California, San Francisco, California*

Accepted for publication July 26, 2021.

Address correspondence to Max Levin, M.D., Department of Oncology, Sahlgrenska University Hospital, Blå Stråket 6, SE-413 45, Göteborg, Sweden. E-mail: max.levin@wlab.gu.se.

Angiogenesis supplies oxygen and nutrients to growing tumors. Inhibiting angiogenesis may stop tumor growth, but vascular endothelial growth factor inhibitors have limited effect in most tumors. This limited effect may be explained by an additional, less vascular endothelial growth factor—driven form of angiogenesis known as intussusceptive angiogenesis. The importance of intussusceptive angiogenesis in human tumors is not known. Epifluorescence and confocal microscopy was used to visualize intravascular pillars, the hallmark structure of intussusceptive angiogenesis, in tumors. Human malignant melanoma metastases, patient-derived melanoma xenografts in mice (PDX), and genetically engineered v-raf murine sarcoma viral oncogene homolog B1 (BRAF)-induced, phosphatase and TENsin homolog deleted on chromosome 10 (PTEN)-deficient (BPT) mice (*Braf*$^{CA/+}$*Pten*$^{f/f}$Tyr-*Cre*$^{+/0}$-mice) were analyzed for pillars. Gene expression in human melanoma metastases and PDXs was analyzed by RNA sequencing. Matrix metalloproteinase 9 (MMP9) protein expression and T-cell and macrophage infiltration in tumor sections were determined with multiplex immunostaining. Intravascular pillars were detected in human metastases but rarely in PDXs and not in BPT mice. The expression of MMP9 mRNA was higher in human metastases compared with PDXs. High expression of MMP9 protein as well as infiltration of macrophages and T-cells were detected in proximity to intravascular pillars. MMP inhibition blocked formation of pillars, but not tubes or tip cells, *in vitro*. In conclusion, intussusceptive angiogenesis may contribute to the growth of human melanoma metastases. MMP inhibition blocked pillar formation *in vitro* and should be further investigated as a potential anti-angiogenic drug target in metastatic melanoma. *(Am J Pathol 2021, 191: 2023—2038; https://doi.org/10.1016/j.ajpath.2021.07.009)*

Tumor growth requires formation of new blood vessels, a process known as angiogenesis. New blood vessels supply the growing tumor with oxygen and nutrients. Consequently, inhibiting angiogenesis may starve cancer cells and prevent cancer progression.[1] Inhibiting angiogenesis is an attractive clinical strategy for two reasons. First, all solid tumors, irrespective of histology or mutation profile, are dependent on angiogenesis. Therefore, angiogenesis inhibition could be universally applicable. Second, adverse effects would be expected to be mild because physiological angiogenesis is relatively rare in adults.[2] Unfortunately, clinical trials with angiogenesis inhibitors have been disappointing.[3,4] One possible explanation for the limited

Supported by the Swedish state under the agreement between the Swedish government and the county councils, the Avtal om Läkarutbildning och Forskning (ALF) agreement (M.L., M.O.B., J.A.N., and S.B.), Jubileumsklinikens Cancerfond, Lions Cancerfond, Stiftelsen Tornspiran, Kungliga och Hvitfeldtska Stiftelsen, Stiftelsen Assar Gabrielssons Fond, Wilhelm och Martina Lundgrens Vetenskapsfond, Serena Ehrenströms Fond, Torsten och Sara Janssons Fond, and NIH National Institute of Diabetes and Digestive and Kidney Diseases grant R01DK74398 (K.E.M.).

Disclosures: None declared.

https://doi.org/10.1016/j.ajpath.2021.07.009

effect of current angiogenesis inhibitors is that only one type of angiogenesis is targeted when there are, in fact, at least two types of angiogenesis.[5]

Sprouting angiogenesis, the classic form of angiogenesis known for >150 years, is the outgrowth of a new vessel branch from an existing vessel. Sprouting angiogenesis is initiated when hypoxic cells secrete vascular endothelial growth factor (VEGF) and other angiogenic factors. VEGF is sensed by specialized tip cells that guide the growing vessel branch toward the most hypoxic cells to restore oxygen supply.[6–8] Current angiogenesis inhibitors target the VEGF pathway and shrink tumors in many mouse models. However, in most human cancers, VEGF-targeted angiogenesis inhibitors either have no effect or only transiently reduce tumor size.[3]

In contrast to sprouting angiogenesis, intussusceptive angiogenesis is understudied and remains enigmatic. Intussusceptive angiogenesis is a remodeling process in which one vessel splits into two parallel vessels. Intussusceptive angiogenesis starts with the formation of a slender endothelial pillar through the vessel lumen. The pillars widen and merge to form a wall through the vessel that divides the single lumen into two parallel lumens.[9] Intussusceptive angiogenesis was first described in 1986 as a mechanism that rapidly expands the vascular networks in the lungs of postnatal rats.[10,11] Since then, intussusceptive angiogenesis has been demonstrated in a range of organs during embryonic and postnatal growth,[12] in chronic inflammation,[13,14] and in lungs of patients with coronavirus disease 2019–induced respiratory failure.[15] The role of intussusceptive angiogenesis in human cancer is almost completely unknown, but it has been described in cancer models.[16–18] Interestingly, intussusceptive angiogenesis may not rely on VEGF and has even been shown to increase during VEGF inhibition in experimental tumors.[19,20]

Metastatic malignant melanoma is an aggressive disease with poor prognosis. Melanoma metastases are rich in angiogenesis and often fast growing. Despite their dependence on angiogenesis for growth, melanoma metastases respond poorly to VEGF-targeted anti-angiogenic therapy.[21,22] This could be explained by untargeted intussusceptive angiogenesis. The aim of the current study was to investigate whether intussusceptive angiogenesis occurs in human metastatic melanoma and in mouse melanoma models. A second aim was to identify mechanisms required for intussusceptive angiogenesis to define new strategies for inhibition.

Materials and Methods

Ethics

All research was performed in accordance with the Declaration of Helsinki of the World Medical Association. Study approval was obtained from the Gothenburg Regional Ethics Committee, and patients gave written informed consent to participate (numbers 151-16 and 288-12). Animal studies were performed in accordance with European Union directive 2010/63 and approved by the Animal Ethics Committee at the University of Gothenburg (number 36-2014).

Human Melanoma Metastases

Fourteen biopsies of cutaneous melanoma metastases were obtained from patients treated for metastatic melanoma at Sahlgrenska University Hospital (Gothenburg, Sweden). Of these, six biopsies (Table 1) were paraffin embedded, sectioned with 6-μm thickness, and stained with hematoxylin and eosin and immunofluorescence. An additional eight surgical biopsies were collected for more detailed three-dimensional analyses. These biopsies were embedded in OCT, flash frozen in liquid nitrogen, and stored at −80°C. The frozen biopsies were sectioned into 20- or 40-μm thickness and stained with immunofluorescence.

Patient-Derived Melanoma Xenografts in Mice and *Braf*$^{CA/+}$*Pten*$^{f/f}$Tyr-*Cre*$^{+/0}$Mice

To establish patient-derived melanoma xenografts (PDXs), melanoma cells from human metastases were mixed with Matrigel (Thermo Fisher Scientific, Waltham, MA) and injected subcutaneously into the flanks of nonobese severe combined immune-deficient IL-2 chain receptor γ knockout mice (Taconic, Ry, Denmark) to form xenografts.[23] *Braf*$^{CA/+}$*Pten*$^{f/f}$Tyr-*Cre*$^{+/0}$mice (BPT mice) is a model in which a

Table 1 Clinical Data of Cutaneous Human Melanoma Metastases Analyzed for Pillars

Sample no.	Sex	Age, years*	BRAF status	Previous/ongoing systemic treatment	Location of cutaneous metastasis	Pillars
1	F†	74	V600E	BRAF inhibitor	Abdomen	Yes
2	F	83	Not analyzed	None	Inguinal	Yes
3	M	52	V600E	BRAF inhibitor, alkylating chemotherapy	Shoulder	Yes
4	M	58	V600E	None	Abdomen	Yes
5	M	78	Wild type	None	Thorax	Yes
6	F†	74	V600E	BRAF inhibitor	Abdomen	Yes

*At the time of sampling.
†Same patient, two different biopsies taken with 5 months' difference.
F, female; M, male; BRAF, v-raf murine sarcoma viral oncogene homolog B1.

genetic trigger is activated to generate primary tumors in the skin, after which spontaneous lymph node metastases develop.[24,25] Paraffin sections (6 μm thick) from flank tumors in the PDX model ($n = 6$) and lymph node metastases from BPT mice ($n = 8$) were obtained and stained with hematoxylin and eosin and processed for immunofluorescence.

Histology and Immunofluorescence

Paraffin-embedded sections were deparaffinized, and heat-induced epitope retrieval in citrate was performed. Frozen sections were fixed in 2% paraformaldehyde for 5 minutes. Sections were either stained with hematoxylin and eosin or labeled using immunofluorescence. Some sections used for immunofluorescence were permeabilized in 0.1% Triton X-100 for 5 minutes, and blocked with 1% bovine serum albumin and 0.3 mol/L glycine in phosphate-buffered saline for 30 minutes. Avidin/streptavidin blocking was performed, and primary antibodies were added (Table 2) in 4°C overnight. After washing, secondary antibodies ($n = 3$) were added for 2 hours, followed by additional washing and mounting of sections with Prolong Gold (Thermo Fisher Scientific). Other sections were stained using a multiplex immunofluorescence assay (Opal Multiplex staining system; Akoya Biosciences, Marlborough, MA), after deparaffinization, antigen retrieval (heat-induced epitope retrieval in Tris buffer), and protein blocking (3% peroxidase and 2% bovine serum albumin). Primary antibodies (Table 2), diluted in 2% bovine serum albumin, were added to the tissue samples for 60 minutes at room temperature on a movable plate. Following a wash in Tris-buffered saline buffer, the slides were incubated with the secondary horseradish peroxidase conjugate for 10 minutes. After a new washing cycle, the slides were incubated with the corresponding Opal fluorophore diluted in ready-to-use tyramide amplification buffer for 10 minutes. The slides were then put into a plastic holder containing Tris-buffered saline buffer and placed in the microwave at 800 W for 40 seconds, followed by 90 W for 15 minutes. When the slides had cooled to room temperature, they were washed and underwent a new cycle of primary antibody staining. Slides were counterstained with DAPI once all the primary antibody cycles were finished. Following another round of washing, the slides were mounted with Prolong Gold.

Stained sections were imaged with a Metafer Slide Scanning Platform (MetaSystems GmbH, Altlussheim, Germany) equipped with custom fluorescence filters.[26]

Screening for Intravascular Pillars

High-resolution tumor images were visually inspected for intravascular pillars using VsViewer version 2.1.113 (MetaSystems GmbH). Pillars were identified as endothelial structures with a collagen core and/or α-actin–positive cells surrounded by endothelium. In human metastases and PDXs, all vessels located intratumorally and peritumorally (250 μm beyond the tumor margin) were individually visually inspected for the presence of intravascular pillars. To distinguish true pillars from folds or artifacts, cross-sections

Table 2 Antibodies Used for Immunofluorescence Staining of Human and Mouse Material

Target	Species	Dilution	Catalog no.; manufacturer
UEA-1, biotinylated	N/A (lectin)	1:200	B-1065; Vector Laboratories, Burlingame, CA
Isolectin B4, biotinylated	N/A (lectin)	1:200	L2140; Sigma Aldrich, St. Louis, MO
CD31	Goat	1:200	AF 3628; R&D Systems, Minneapolis, MN
α-Actin, cy3	Mouse	1:1000	C6198; Sigma Aldrich
Collagen I	Mouse	1:100	Ab6308; Abcam, Cambridge, UK
Collagen IV	Rabbit	1:200	Ab6586; Abcam
MMP9	Mouse	1:200	NBP1-28617B; Novus Biologicals, Littleton, CO
MMP9	Mouse	1:100	SMC-396D-BI; StressMarq, Cadboro Bay, CA
MMP9	Rabbit	1:200	ab228402; Abcam
Mac2/Galactin-3	Rat		125,412; Biolegend, San Diego, CA
CD68	Mouse	1:100	Ab 955; Abcam
Ki-67	Mouse	1:400	M7240; Dako, Copenhagen, DK
CD3	Rabbit	RTU	IR503; Dako
Atto425	N/A (streptavidin)	1:100	AD 425-61; ATTO-TEC,Siegen, DE
Mouse IgG, Alexa 488	Donkey Fab'	1:400	715-547-003; Jackson Immunoresearch, Cambridge, UK
Rabbit IgG, Alexa 594	Donkey Fab'	1:400	711-587-003; Jackson Immunoresearch
Goat IgG, Alexa 647	Donkey Fab'	1:200	705-607-003; Jackson Immunoresearch
CF 594 tyramide		1:100	Number 92174; Biotium, Fremont, CA
CF 488A tyramide		1:200	Number 92171; Biotium
CF 555 tyramide		1:200	Number 96021; Biotium

MMP, matrix metalloproteinase; N/A, not applicable.

of suspected pillars were performed using confocal microscopy. Tumor area (mm^2) and vessel and pillar densities (number/mm^2) were quantified for all samples.

Gene Expression Analysis

RNA was prepared from patient ($n = 11$) and PDX biopsies ($n = 26$), as described previously.[23,27,28]

Alignment and Preprocessing of RNA-Sequencing Data

RNA reads were aligned to the hg38 human and to the GRCm38 mouse reference genome assembly using STAR version 2.7.1a,[29] with splice junctions supplied from the hg38 GENCODE2[30] version 27 human and GENCODE version M22 mouse reference annotation, respectively, using the parameters "–twopassMode Basic -outSAMmapqUnique 60" and "–sjdbOverhang 75" or "–sjdbOverhang 125", depending on sequencing batch. For PDX samples, reads deriving from human were retrieved using Disambiguate version 1.0,[31] with the parameter "-a star".

Estimation of Gene Expression Levels

Aligned reads were binned to genes using htseq-count, (HTSeq version 0.11.2),[32] with respect to the GENCODE version 27 reference genome annotation, using the parameters "-r name -q -f bam -m intersection-strict" and "-s reverse", "-s yes," or "-s no", depending on sequencing batch.

MMP9, Macrophages, and T Cells in Human and Mice Melanoma

High-resolution tumor images were analyzed to quantify matrix metalloproteinase 9 (MMP9), macrophages, and T cells adjacent to blood vessels with or without pillars in human melanoma metastases. First, blood vessels with verified pillars were identified. The blood vessels were analyzed for proliferating endothelial cells, defined as colocalization of endothelial cell marker ulex europaeus agglutinin I (UEA-1) and Ki-67 staining. MMP9, macrophages, and T cells were quantified in an area around the specified pillar containing vessels, corresponding to a region of interest of 1.23 mm^2. Areas without pillars, nonpillar zones, were analyzed in the same way. In mice tumors, MMP9, macrophages, and T cells adjacent to blood vessels were analyzed using the same technique.

Table 3 TaqMan Probes Used for qPCR

Target	Assay ID
MMP1	Hs00899658_m1
MMP2	Hs01548727_m1
MMP3	Hs00968305_m1
MMP9	Hs00957562_m1
MMP10	Hs00233987_m1
MMP11	Hs00968295_m1
MMP12	Hs00159178_m1
MMP13	Hs00942584_m1
MMP14	Hs01037003_g1
ACTB	Hs01060665_g1

ACTB, ActinBeta; ID, identifier; MMP, matrix metalloproteinase; qPCR, real-time quantitative PCR.

In Vitro Models of Pillar and Tube Formation

Two cell co-culture models were used to study either pillar or tube and tip cell formation *in vitro*.[33] The first model has features of intussusceptive angiogenesis (pillars) and the second model has features of both vasculogenesis (*de novo* formation of blood vessels) and sprouting angiogenesis (tip cell formation). In both models, human pulmonary artery smooth muscle cells (100,000 cells/cm^2; Lonza number CC-2581; Thermo Fisher Scientific) were seeded onto a Transwell polyester membrane insert (number 3460; Corning, Corning, NY). After 24 hours,

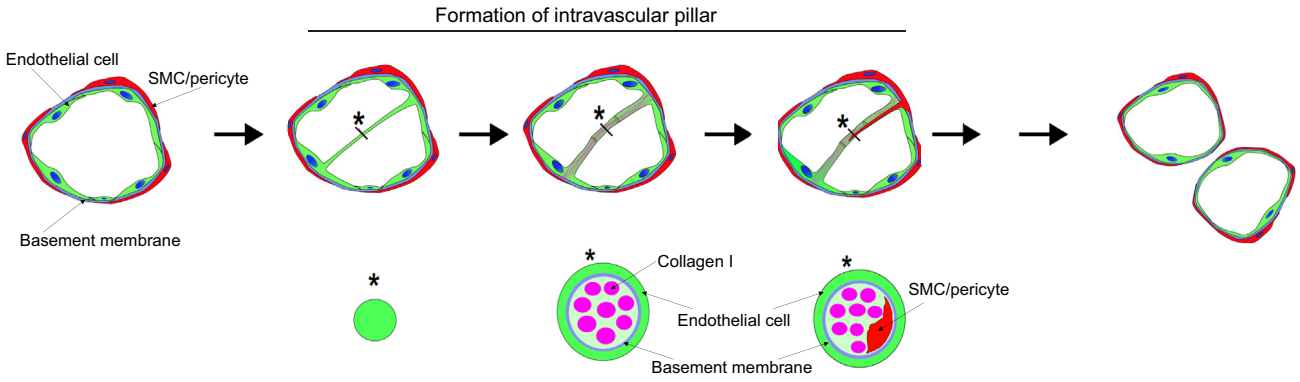

Figure 1 Intravascular pillar: the hallmark structure of intussusceptive angiogenesis. The first step in intussusceptive angiogenesis is that endothelial cells extending from opposing sides of a vessel lumen fuse to form a slender pillar. Then, the pillar develops a core of collagen I and collagen IV, and finally, smooth muscle cells (SMCs) or pericytes migrate into the widening pillar. Several pillars are formed downstream of the initial pillar, and as they fuse together, the vessel is split into two parallel vessels. **Asterisks** indicate cross-section of pillars.

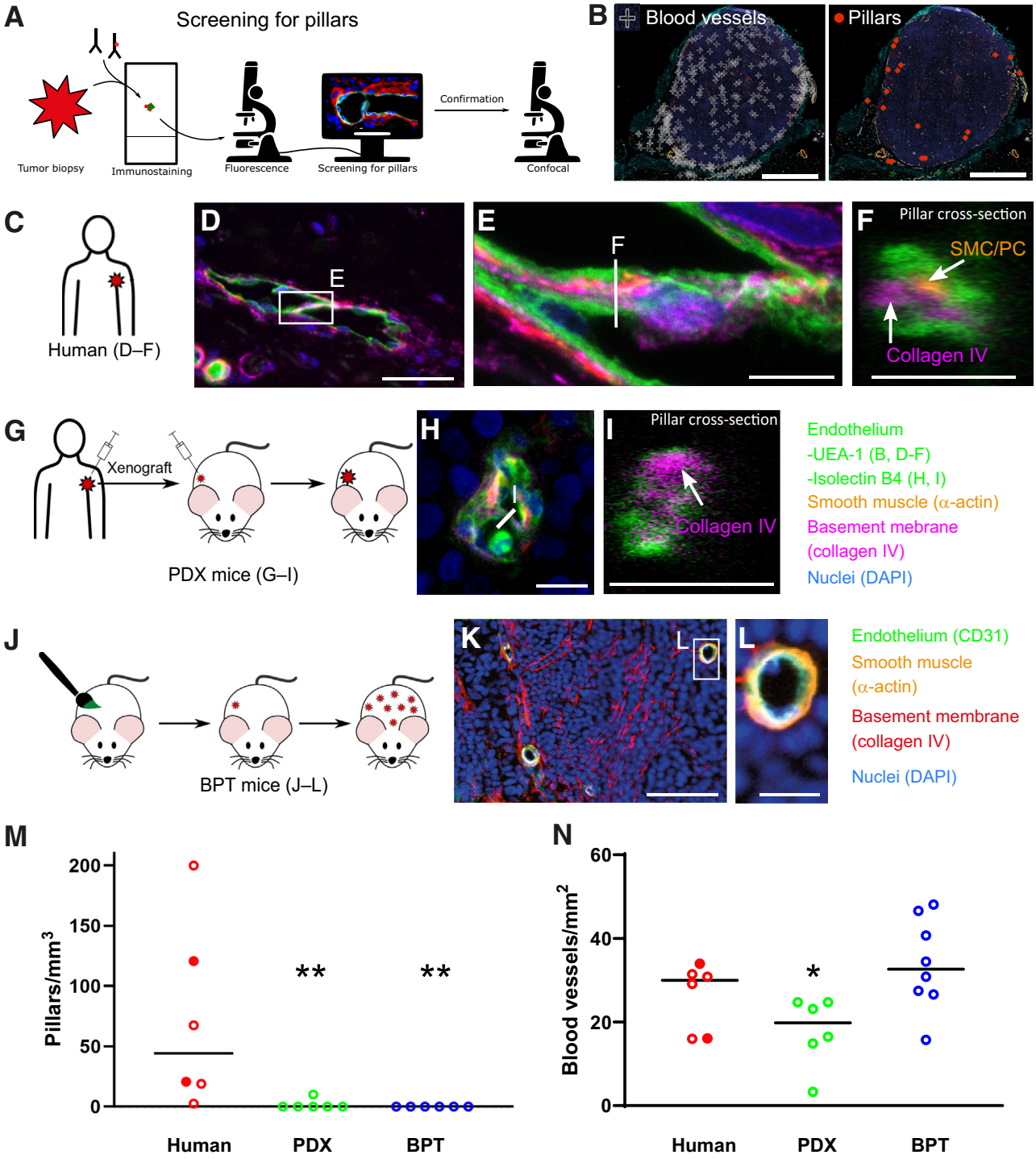

Figure 2 Intravascular pillars are common in human melanoma metastases and rare in mouse melanoma models. **A:** Tumor sections were immunostained with fluorescently labeled antibodies and scanned. Every blood vessel was visually inspected for suspected intravascular pillars. Three-dimensional confirmation of suspected pillars was performed using serial confocal microscopy and subsequent reconstruction of pillar cross-sections. **B:** Scanned tumor section (human metastasis); all blood vessels (cross) within the sections were examined for intravascular pillars (red dot). **C**—**F:** Intravascular pillars were found in all human metastases analyzed. Intravascular pillars consisted of an outside of endothelial cells with a core of collagen IV and smooth muscle cells/pericytes (SMCs/PCs). **G**—**I:** Intravascular pillars were only detected in one of six patient-derived melanoma xenograft in mice (PDX) tumors but had a similar structure as in human metastases. **J**—**L:** No intravascular pillars were detected in metastases from BRAF-induced, PTEN-deficient (BPT) mice. **M:** There were significantly more pillars in human metastases than in the mouse models. The closed red dots represent two different metastases in one patient. The biopsies were taken at different time points. **N:** There was no significant difference in vessel density between human and mouse tumors but significantly higher vessel density in BPT versus PDX mice. The closed red dots represent two different metastases in one patient. The biopsies were taken at different time points. **M** and **N:** Analysis of variance with the Tukey multiple comparisons test was performed. $n = 6$ (**C**—**F**); $n = 8$ (**J**—**L**). $^{*}P < 0.05$, $^{**}P < 0.01$ versus human. Scale bars: 2 mm (**B**); 30 μm (**D**); 5 μm (**E**, **F**, and **I**); 10 μm (**H** and **L**); 40 μm (**K**). BRAF, v-raf murine sarcoma viral oncogene homolog B1; PTEN, phosphatase and TENsin homolog deleted on chromosome 10.

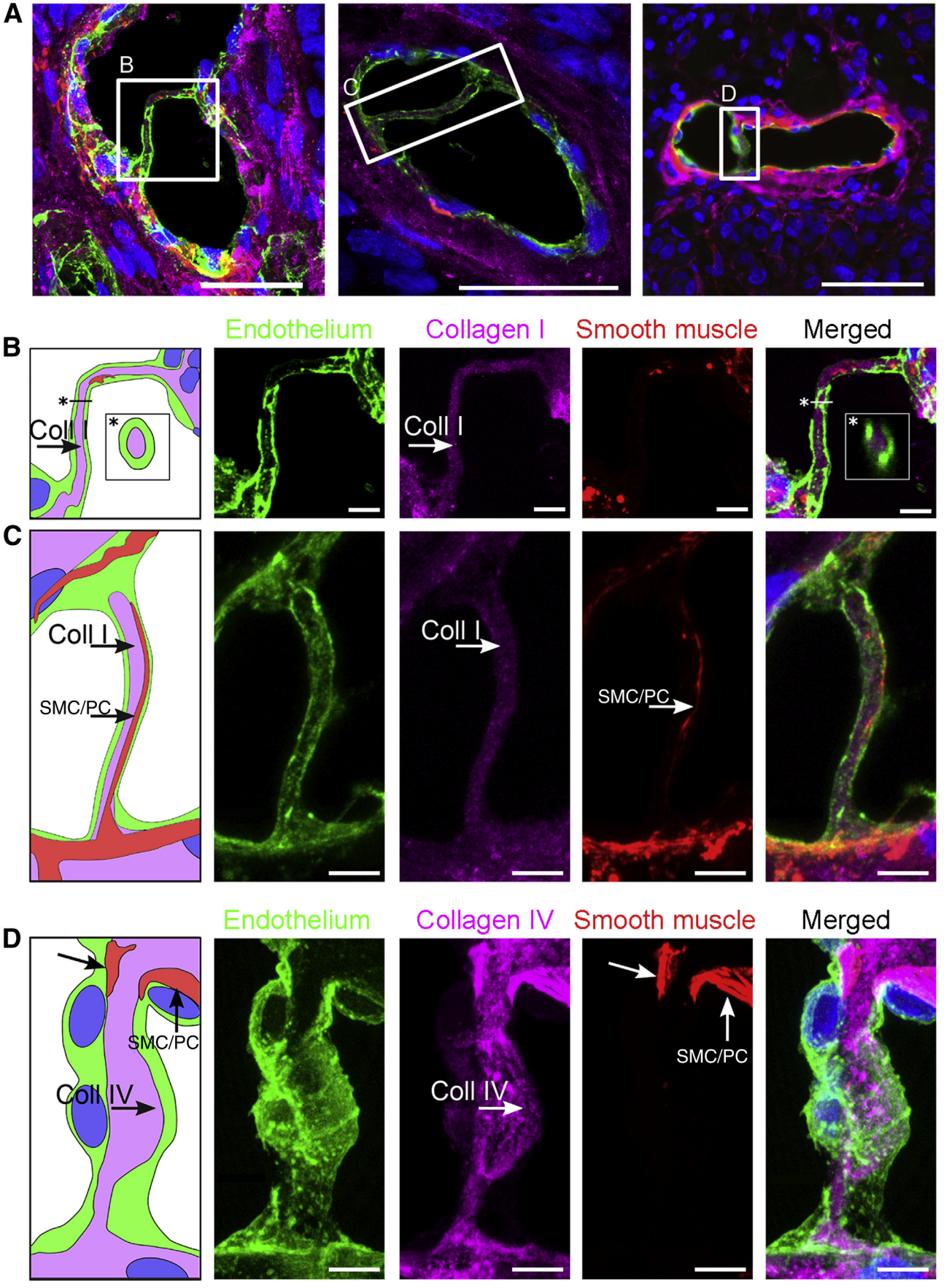
A
B
C
D
Endothelium
Collagen I
Smooth muscle
Merged
B
Coll I
*
C
Coll I
SMC/PC
D
Endothelium
Collagen IV
Smooth muscle
Merged
SMC/PC
Coll IV

telomerase-immortalized microvascular endothelial cells (ATCC CRL-4025; ATCC, Manassas, VA) were added on top of the smooth muscle cells. A high density of telomerase-immortalized microvascular endothelial cells (50,000/cm^2) was added on top of the smooth muscle cells to form pillars, and a low density of telomerase-immortalized microvascular endothelial cells (10,000/cm^2) was added to form tubes and tip cells. Medium (EGM2-MV; Lonza, CC-3202; Thermo Fisher Scientific) was changed every second day. The membranes with cells were fixed in 4% paraformaldehyde for 30 minutes, and stored in 0.1% paraformaldehyde until staining of whole filters in the same manner as described above, with the addition of 0.1% saponin during antibody incubations. To investigate the effect of broad-spectrum MMP inhibition on pillar formation, MMP inhibitor batimastat (BB94; British Biotech, Oxford, UK) or ilomastat (Sigma Aldrich, St. Louis, MO) was added to the cell culture medium.

Expression of MMP mRNAs in Pillar Co-Culture Model

mRNA expression of MMPs was analyzed in pillar co-cultures as well as in single cultures of smooth muscle cells or endothelial cells. Isolation of mRNA was performed after 7 days using an RNeasy minikit (Qiagen, Hilden, Germany). cDNA was produced using a High-Capacity cDNA reverse transcription kit (4368813; Applied Biosystems, Foster, CA) with random primers. mRNA expression of the genes of interest was analyzed through a TaqMan real-time PCR in a ViiA 7 system (Thermo Fisher Scientific) with the primers listed in Table 3, using ActinBeta (ACTB) as an internal control.

Live Cell Confocal Microscopy

To investigate if MMP inhibition reduces movement of smooth muscle cells in pillars, live-cell confocal microscopy was used. Smooth muscle cells were marked with Celltracker orange (Thermo Fisher Scientific), and endothelial cells were marked with Celltracker green (Thermo Fisher Scientific). The cells were grown in 96-well cover glass bottom plates (Thermo Fisher Scientific) for 7 days to form pillars. Then, MMP inhibitor batimastat (50 μmol/L; Sigma Aldrich) or vehicle (dimethyl sulfoxide) was added, and smooth muscle cell movement during 24 hours was quantified using live-cell imaging. Live-cell imaging was performed on a custom spinning disk confocal microscope system (Solamere Technology Group, Salt Lake City, UT). Briefly, the system was built around a Zeiss Axiovert 200 M microscope (Zeiss, Oberkochen, Germany), a Yokogawa CSU-10 confocal (Yokogawa, Sugar Land, TX), argon and krypton lasers from Dynamic Lasers (Salt Lake City, UT), a Blue Sky 405 solid state laser (Blue Skye Research, Milpitas, CA), an Applied Scientific Instruments (Eugene, OR) MS-2000 motorized stage, and an Applied Scientific Instruments FW-1000 filter wheel. Zeiss Fluar (10× to 40×), LD-Plan Neofluar (20× to 40×), and LD-LCI C-Apochromat (40×) objective lenses were used (Carl Zeiss, Oberkochen, Germany). Image collection relied on QED *In Vivo* (Media Cybernetics, Rockville, MD). Image analysis was performed using Imaris version 4.1 (Bitplane, Belfast, UK). Environmental control was achieved using a custom-built enclosure and a World Precision Instruments Air Therm ATX (Sarasota, FL).

Statistical Analysis

The *t*-test for unpaired data or analysis of variance with Tukey multiple comparisons or Holm-Šídák test was performed to assess significance, and $P < 0.05$ was considered significant. Differentially expressed genes between human biopsies and PDX samples were assessed using DESeq2 version 1.26.0[34] with the parameter "alpha = 0.05" in R version 3.6.1 (R Foundation for Statistical Computing, Vienna, Austria; *https://www.r-project.org*), accounting for sequencing batch. False discovery rate–adjusted *P* values were calculated using the Benjamini-Hochberg method, and $P < 0.05$ was considered statistically significant.

Results

Intravascular Pillars Are Frequent in Human Melanoma Metastases

Intussusceptive angiogenesis starts with the formation of intravascular pillars (Figure 1). To investigate if intussusceptive angiogenesis occurs in human melanoma, human metastases ($n = 6$) were scanned for pillars (Figure 2). Pillars were detected in all six metastases examined (Figure 2) and were mainly observed in the periphery of the metastases. To perform detailed structural characterization of pillars, thick cryosections of flash-frozen human melanoma metastases ($n = 8$) were analyzed using confocal microscopy. Pillars in different stages of maturation were detected with this approach (Figure 3). Pillars were 2 to 5 μm in diameter and consisted of endothelial cells with an

Figure 3 Structure of intravascular pillars in human melanoma metastases. **A:** Three different intravascular pillars within blood vessels in human melanoma metastases. **B–D:** Detailed structure of each pillar is shown. Intravascular pillar stained for endothelium (UEA-1; green), collagen I (Coll I; purple), and α-actin (red) (**B**). Note the endothelial coating with a collagen I core throughout the pillar. **Asterisks** indicate level of the pillar cross-section that is shown in the inserted box. Identically stained pillar, in which an extension from an adjacent smooth muscle cell/pericyte (SMC/PC) projects into the pillar core (**C**). Pillar stained for basement membrane protein collagen IV (Coll IV) in the purple channel (**D**). The presence of collagen IV suggests remodeling of the basement membrane during pillar formation. Also note the smooth muscle cells/pericytes extending, possibly migrating into, the pillar. Scale bars: 25 μm (**A**); 5 μm (**B–D**).

Table 4 Morphologic Features of the Human and Mice Tumors

Morphologic feature	Human	PDX model	BPT model
Vascularization	++	+	++
Inflammation	++	+	+
Necrosis	++	+	−
Cell density	++	++	+
Stroma	+	+	++

Assessment by a pathologist.
+, Present; ++, pronounced; −, not present; BRAF, v-raf murine sarcoma viral oncogene homolog B1; BPT, BRAF-induced, PTEN deficient; PDX, patient-derived melanoma xenografts in mice; PTEN, phosphatase and TENsin homolog deleted on chromosome 10.

underlying basement membrane (collagen type IV) and a collagen type I core (Figure 3). α-Actin–positive pericytes/smooth muscle were present inside mature pillars (Figure 3). There was less proliferation in endothelial cells in blood vessels with pillars compared with blood vessels without pillars (16.8% ± 7.5% versus 28.8% ± 9.2%; $P = 0.033$, *t*-test). Taken together, these data demonstrate the presence of intravascular pillars in human melanoma metastases. Pillars were common in viable peripheral parts of the tumor and rare in central necrotic and perinecrotic areas. The presence of pillars in melanoma metastases suggests that intussusceptive angiogenesis may promote expansion of the vascular network during tumor growth. Taken together, pillars were detected in all human samples, often in the peripheral parts of the metastases and with lower percentages of proliferation endothelial cells compared with non-pillar zones.

Intravascular Pillars Are Rare in PDX and BPT Mice

The next aim was to establish an experimental melanoma model to study mechanisms of pillar formation and how intussusceptive angiogenesis contributes to tumor growth. Therefore, intravasular pillars were analyzed in two

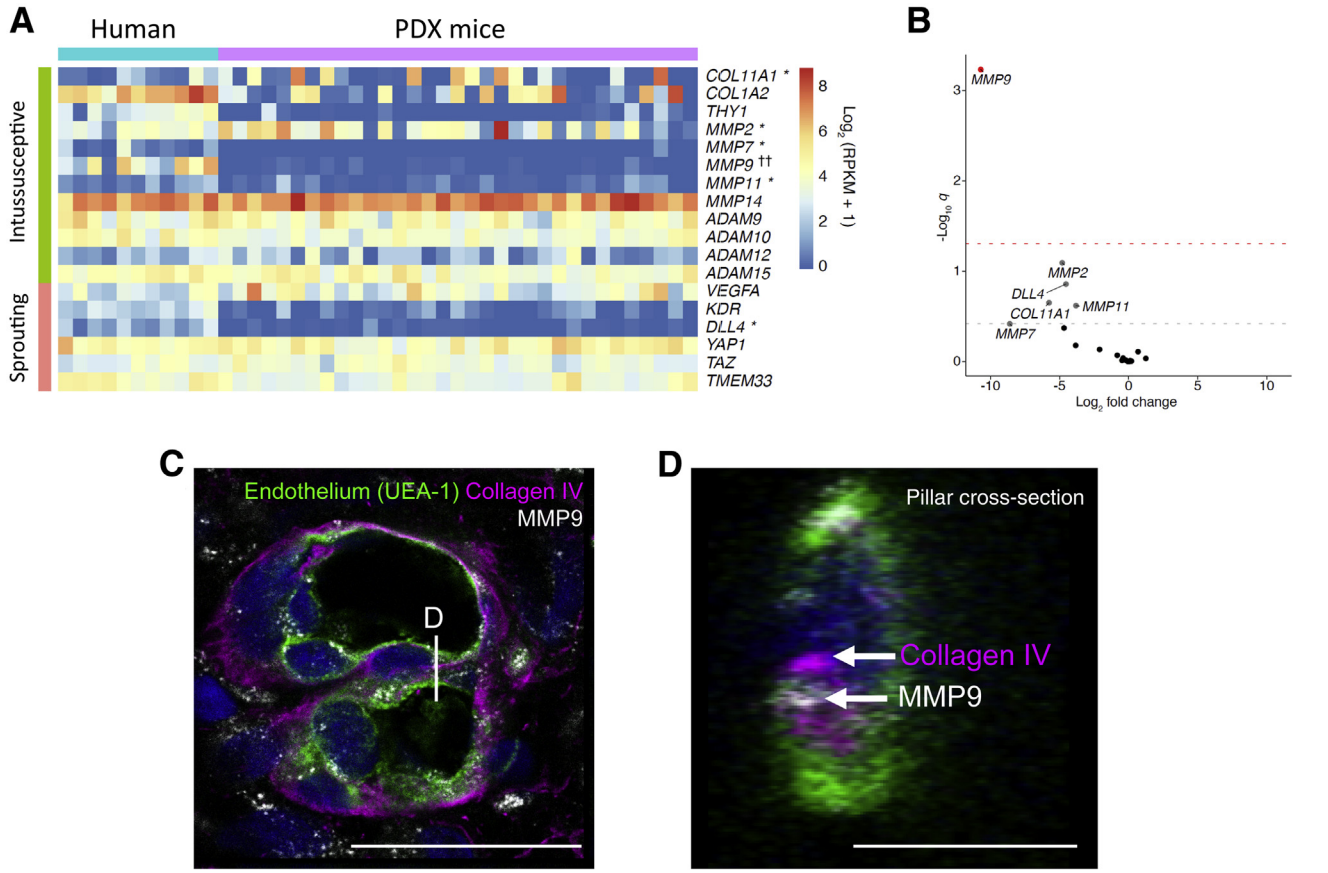

Figure 4 Higher expression of matrix metalloproteinase 9 (MMP9) mRNA in human metastases than in patient-derived melanoma xenografts in mice (PDX). **A:** RNA-sequencing data on human melanoma metastases and patient-derived melanoma xenografts in mice. **B:** MMP9 expression was significantly higher in human metastases after false discovery rate correction ($q < 0.05$; Benjamini-Hochberg method; significance level indicated by **red dashed line**). MMPs 2, 7, and 11 were nominally higher expressed ($P < 0.05$; indicated by **gray dashed line**), as were collagen 11 and Delta-like ligand 4 (DLL4). **C:** Section of s.c. human melanoma metastasis stained for endothelium (UEA-1; green), collagen IV (purple), and MMP9 (white). Note MMP9 positivity in endothelial and perivascular cells. **D:** Enlargement of intravascular pillar, showing MMP9 expression within the pillar and colocalization with basement membrane protein collagen type IV, an MMP9 substrate. $n = 11$ human melanoma metastases (**A**); $n = 33$ PDXs (**A**). *$P < 0.05$ (unadjusted); ††$q < 0.05$ (Benjamini-Hochberg adjusted). Scale bars: 25 μm (**C**); 5 μm (**D**). RPKM, reads per kilobase of transcript, per million mapped reads.

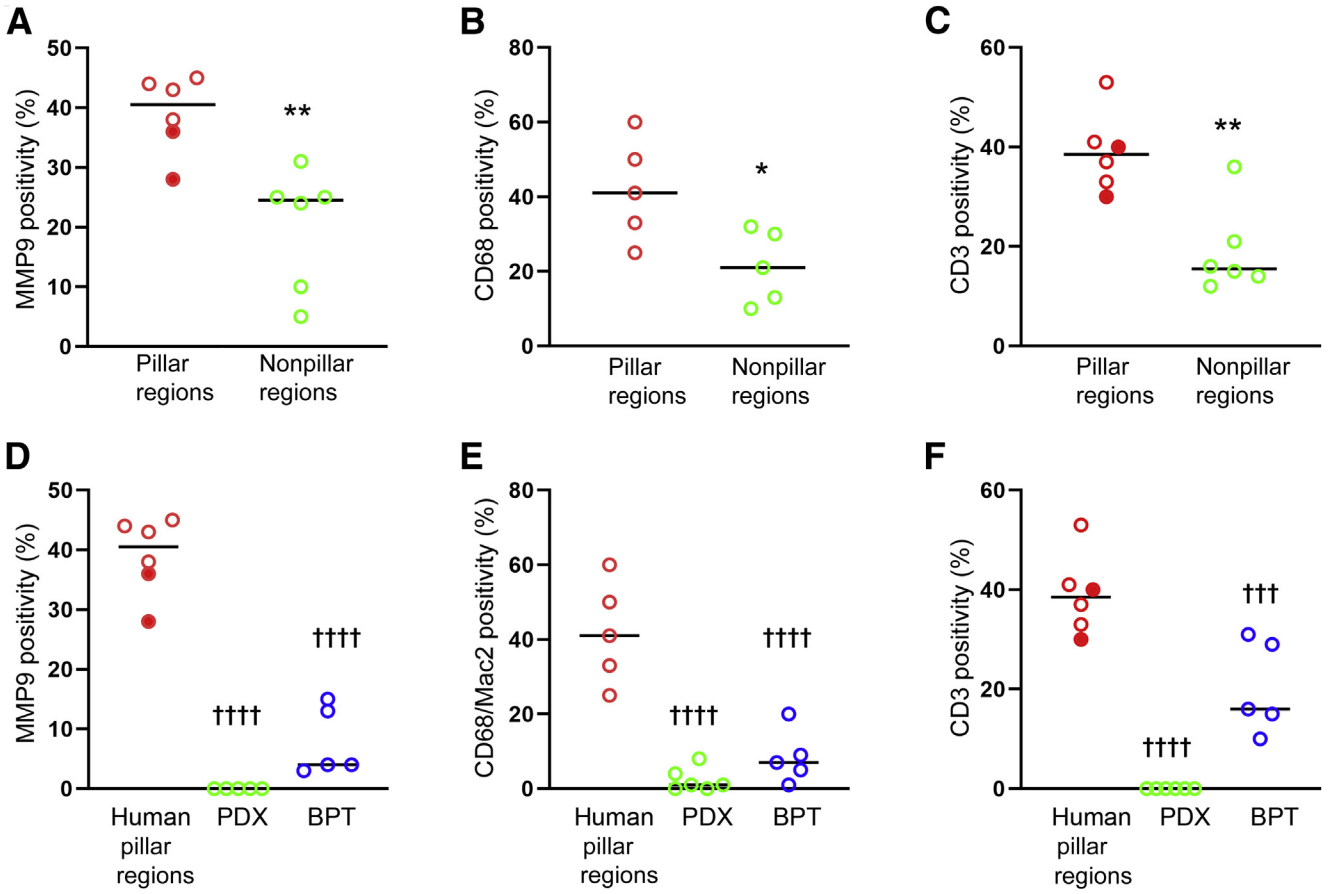

Figure 5 Higher perivascular matrix metalloproteinase 9 (MMP9) expression, more macrophages, and more $CD3^+$ T cells in regions with intussusceptive angiogenesis. **A:** The perivascular expression of MMP9 was higher in regions of human metastases with intussusceptive pillars than in regions without pillars. **B** and **C:** There were more perivascular macrophages (**B**) and $CD3^+$ T cells (**C**) in regions with pillars than in regions without pillars. **A**—**C:** The *t*-test was used. **D**—**F:** There was less MMP9 expression and lower numbers of perivascular macrophages and $CD3^+$ T cells in patient-derived melanoma xenografts in mice (PDX) and BRAF-induced, PTEN-deficient (BPT) mice than in pillar regions of human metastases regions. The closed red dots represent two different metastases in one patient. The biopsies were taken at different time points. **D**—**F:** Analysis of variance with Holm-Šídák test was used. $^*P < 0.05$, $^{**}P < 0.01$ versus pillar regions; $^{\dagger\dagger\dagger}P < 0.001$, $^{\dagger\dagger\dagger\dagger}P < 0.0001$ versus human pillar regions. BRAF, v-raf murine sarcoma viral oncogene homolog B1; PTEN, phosphatase and TENsin homolog deleted on chromosome 10.

different mouse melanoma models: PDX mice and $Braf^{CA/+}Pten^{f/f}$Tyr-$Cre^{+/0}$ (BPT mice). In contrast to human metastases, only one of six samples contained pillars in the PDX model (Figure 2). In lymph node metastases from BPT mice ($n = 8$), no intravascular pillars were detected (Figure 2). In summary, intravascular pillars were rare in PDXs and could not be detected at all in BPT mice. Consequently, intussusceptive angiogenesis is not likely to contribute to tumor growth in these models.

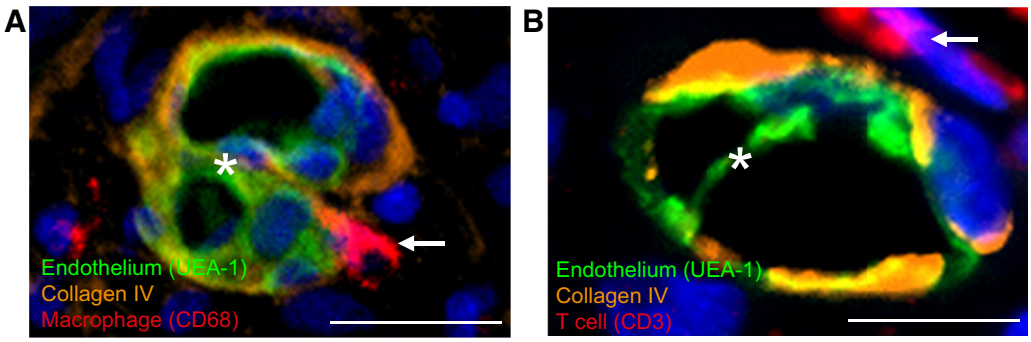

Figure 6 Macrophage and T cell adjacent to intravascular pillars. **A:** $CD68^+$ macrophage (**arrow**) in close proximity to intravascular pillar (**asterisk**). **B:** $CD3^+$ T cell (**arrow**) adjacent to blood vessel with intravascular pillar (**asterisk**). Scale bars: 20 μm (**A**); 15 μm (**B**).

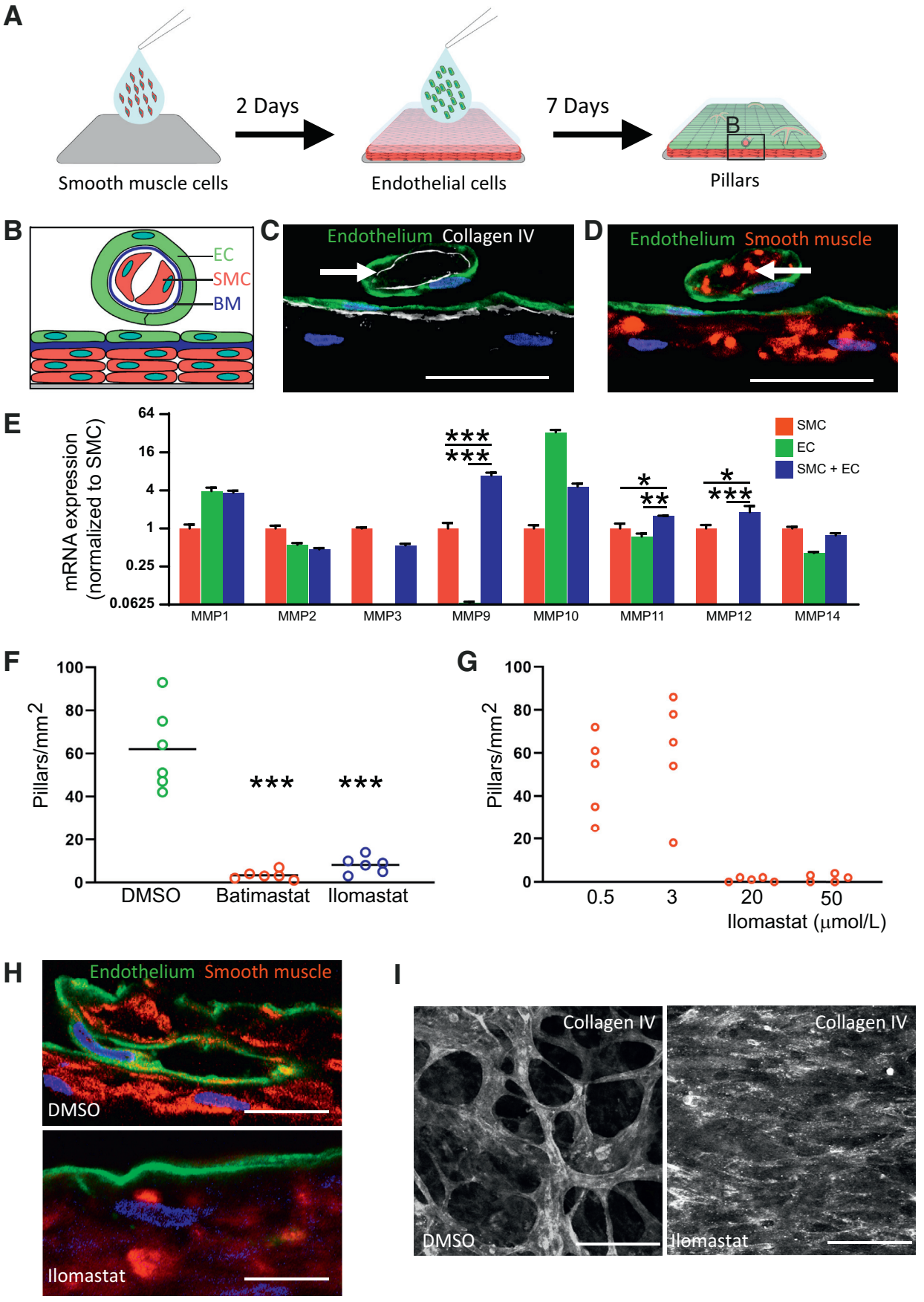
A
2 Days
7 Days
Smooth muscle cells
Endothelial cells
B
Pillars
B
EC
SMC
BM
C
Endothelium Collagen IV
D
Endothelium Smooth muscle
E
mRNA expression (normalized to SMC)
64
16
4
1
0.25
0.0625
SMC
EC
SMC + EC
***
***
*
**
*
***
MMP1
MMP2
MMP3
MMP9
MMP10
MMP11
MMP12
MMP14
F
Pillars/mm2
100
80
60
40
20
0
***
***
DMSO
Batimastat
Ilomastat
G
Pillars/mm2
100
80
60
40
20
0
0.5
3
20
50
Ilomastat (μmol/L)
H
Endothelium Smooth muscle
DMSO
Ilomastat
I
Collagen IV
DMSO
Collagen IV
Ilomastat

More Inflammation in Human Metastases than in Mouse Tumors

The histologic characteristics, as determined by an experienced pathologist (L.M.A.), of the two different models in comparison with human metastases are summarized in Table 4. Human metastases had higher infiltration of inflammatory cells than tumors in PDX and BPT mice. Human metastases and PDXs were otherwise histologically similar, whereas tumors from BPT mice had a lower cellular density, more stroma, and no necrotic areas.

MMP9 Expression Is Higher in Human Melanoma than in Melanoma PDX

Intravascular pillars were detected in human metastases but rarely when cells from human metastases were grown in mice (PDXs). Consequently, differences in gene expression between human metastases and PDXs may reveal genes required for pillar formation. Therefore, a comparison of the gene expression in human melanoma metastases (with pillars) and with PDXs (without pillars) was performed. Figure 4A shows expression levels of genes important in sprouting angiogenesis and intussusceptive angiogenesis, as well as genes involved in remodeling of basement membrane proteins, because formation of intravascular pillars also requires remodeling of the endothelial basement membrane. After false discovery rate correction, one gene, MMP9, was found to be expressed significantly higher in human metastases ($q < 0.05$). MMPs 2, 7, and 11 and Delta-like ligand 4 (DLL4) were nominally significantly higher in human metastases ($P < 0.05$) (Figure 4B). More importantly, MMP9 protein was expressed around blood vessels and within pillars in human melanoma biopsies (Figure 4, C and D). On the basis of this analysis, MMP activity seems to be required for the formation of intravascular pillars.

MMP9, Macrophages, and T Cells Adjacent to Blood Vessels with or without Pillars

More inflammatory cells and higher MMP9 mRNA expression characterized human metastases compared with mouse tumors, suggesting potential roles in intussusceptive angiogenesis. Therefore, human and mouse tumors were stained for MMP9, macrophages, and T cells. In human melanoma metastases, expression of MMP9, macrophages, and T cells was higher adjacent to blood vessels with intussusceptive pillars than in blood vessels without pillars in the same metastases (Figure 5, A–C). Also, MMP9, macrophages, and T cells were more abundant in human metastases than in mouse tumors (Figure 5, D–F). Macrophages and T cells were detected in close proximity to pillars (Figure 6), suggesting a potential role in pillar formation.

Effects of MMP Inhibition on Pillar and Tube Formation *in Vitro*

On the basis of the findings of higher MMPs in human metastases compared with PDXs and BPT mice, the hypothesis that MMP inhibition decreases pillar formation was addressed. For these experiments, a three-dimensional co-culture model was used (Figure 7A).[33] *In vitro* pillars in this model were similar to *in vivo* pillars with an outside of endothelial cells with basement membrane and an inside of smooth muscle cells (Figure 7, B–D). MMP mRNA expression in co-cultures is shown in Figure 7E. Interestingly, MMP9, MMP11, and MMP12 were significantly higher in co-cultures compared with the smooth muscle cells or endothelial cells grown as monocultures. In agreement with the hypothesis, the MMP inhibitor batimastat blocked pillar formation *in vitro*, and similar results were obtained with ilomastat (GM6001), a structurally and mechanistically different MMP inhibitor (Figure 7, F and G). Endothelial cells in co-cultures treated with MMP inhibitors grew as a confluent monolayer on top of the smooth muscle cells but did not form pillars (Figure 7H). The endothelial basement membrane was extensively remodeled during pillar formation but not in co-cultures treated with MMP inhibition (Figure 7I). Collectively, the results indicate that MMP inhibition decreases plasticity of co-cultures and thus prevents pillar formation.

The effect of MMP inhibition on *in vitro* formation of tubes and tip cells was also investigated. The *in vitro* model

Figure 7 Matrix metalloproteinase (MMP) inhibitors stop *in vitro* pillar formation. **A:** To grow pillars, a high density of endothelial cells was added on top of established layers of smooth muscle cells (SMCs). After approximately 7 days, multiple pillars are formed, extending like arches above the monolayer. The **black boxed area** indicates a pillar above the monolayer. **B:** High-resolution images of pillar cross-section. The cartoon shows the principal components of *in vitro* pillars: an outside of endothelial cells (ECs; green) with an underlying basement membrane (BM; blue) and smooth muscle cells (red) inside the pillar. **C:** *In vitro* pillar stained for endothelium (green) and collagen IV. The collagen IV staining demonstrates an endothelial basement membrane inside the pillar (**arrow**). **D:** The same pillar was also stained for smooth muscle cells (red). Smooth muscle cells are present within the core of *in vitro* pillars, similar to mature pillars *in vivo* (**arrow**). **E:** mRNA expression of MMPs in smooth muscle cells (red bar), endothelial cells (green bar), and co-cultures (blue bar). MMP9 mRNA expression and MMP11 expression were higher in pillar co-cultures (SMCs + ECs) than in ECs or SMCs grown in monoculture. **F:** MMP inhibitors batimastat and ilomastat decreased formation of *in vitro* pillars. **E** and **F:** One-way analysis of variance with Holm-Šídák test was used. **G:** Effect of different concentrations of ilomastat on *in vitro* pillar formation. **H:** Cross-section of co-cultures with or without ilomastat. Co-cultures grown without ilomastat formed pillars [dimethyl sulfoxide (DMSO); **top panel**], whereas co-cultures treated with ilomastat grew as a monolayer of endothelial cells on top of smooth muscle cell (Ilomastat; **bottom panel**). **I:** Top view of basement membrane in co-cultures with or without treatment with ilomastat. **Left panel:** The basement membrane inside pillars in co-cultures grown without ilomastat is visualized. **Right panel:** The flat basement membrane between the endothelial and smooth muscle cell layer in co-cultures treated with ilomastat. $*P < 0.05$, $**P < 0.01$, and $***P < 0.001$ versus DMSO. Scale bars: 5 μm (**C**, **D**, and **H**); 80 μm (**I**).

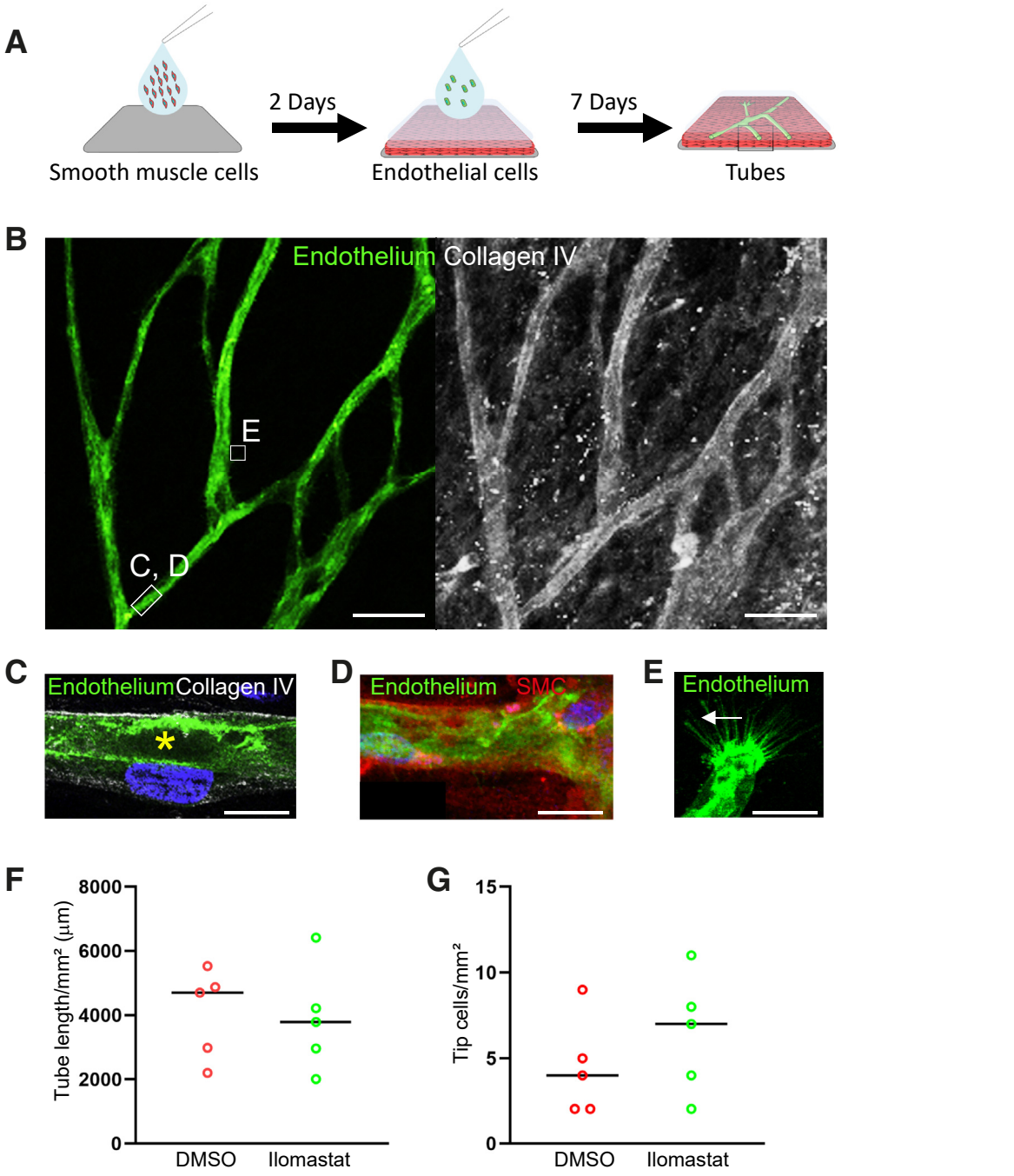

Figure 8 Matrix metalloproteinase (MMP) inhibition does not affect vascular tube or tip cell formation. **A:** To grow vascular tubes and tip cells, a low density of endothelial cells was added on top of established layers of smooth muscle cells (SMCs). A lower number of endothelial cells was added than in pillar co-cultures. The scattered endothelial cells aggregate into vascular-like networks of endothelial tubes. Endothelial cells at the top of blind ending tubes have a typical tip cell phenotype with multiple filopodia (**arrow**). **B:** Top view of vascular tubes, showing a blood vessel—like morphology. **C**—**E:** High-resolution images of the areas indicated by **white boxed areas** in **B**. High-resolution images of vascular tube; note lumen (**asterisk**; **C**), basement membrane, and surrounding smooth muscle cells (**C** and **D**). Detail of endothelial cell at the end of a tube. Note tip cell—like morphology with sprouting filopodia (**arrow**) (**E**). **F** and **G:** MMP inhibition with ilomastat did not affect tube or tip cell formation. One-way analysis of variance with Holm-Šídák test was used. Scale bars: 80 μm (**B**); 10 μm (**C** and **D**); 5 μm (**E**). DMSO, dimethyl sulfoxide.

used had features of both vasculogenesis and sprouting angiogenesis (Figure 8A). *In vitro* tubes were similar to blood vessels with lumen and basement membrane (Figure 8, B and C), and the tubes were surrounded by smooth muscle cells (Figure 8D). Endothelial cells at the end of blind ending tubes had extensive spouting filopodia (Figure 8E). Thus, these cells had a similar phenotype as tip cells formed during sprouting angiogenesis.[8] MMP

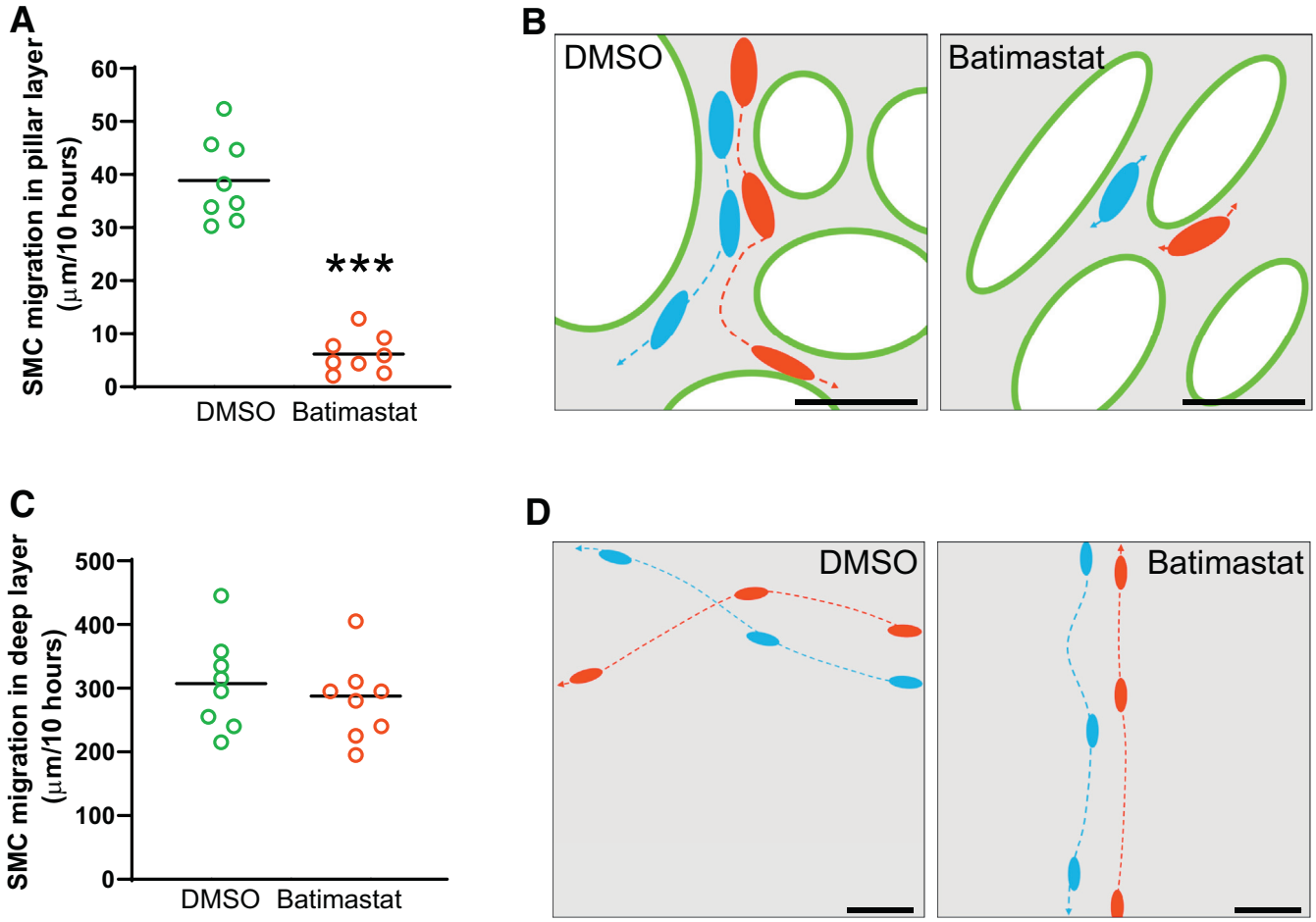

Figure 9 Matrix metalloproteinase (MMP) inhibition decreases smooth muscle cell (SMC) movement in pillars. **A:** MMP inhibition decreased smooth muscle cell migration in pillars (*t*-test). **B:** Migration tracks of smooth muscle cells in pillars with or without MMP inhibition. Each migration track (one red and one blue) shows the migration of a smooth muscle cell over 10 hours. The corresponding movie is available as a supplement (Supplemental Video S1). Note that smooth muscle cells make oscillating movements in cultures with MMP inhibitor but do not migrate. **C:** MMP inhibition had no effect on migration in the deep smooth muscle cell layers of the same co-culture (*t*-test). **D:** Migration tracks from the deep smooth muscle cell layer. Each migration track shows the migration of a smooth muscle cell over 10 hours. Note that smooth muscle cells migrate at similar speed with or without MMP inhibition. Also note the higher migration speed in deep layers compared with pillars. The corresponding movies are available as a supplement (Supplemental Video S2 is without MMP inhibition, and Supplemental Video S3 is with MMP inhibitor). $n = 8$ independent movies (**A** and **C**). $^{***}P < 0.001$ versus DMSO. Scale bars = 50 μm (**B** and **D**). DMSO, dimethyl sulfoxide.

inhibition had no effect on either tube or tip cell formation in this model (Figure 8, F and G).

Effect of MMP Inhibition on Smooth Muscle Cell Movement in Pillar Co-Cultures

Live cell imaging was performed to further investigate the potential effects of MMP inhibition on plasticity during pillar formation. The 24-hour live cell time-lapse confocal movies were made to track smooth muscle cell movement in co-cultures with or without the addition of batimastat. The movies were obtained from two different confocal planes, the level of pillars and the deep smooth muscle cell layer just above the cover glass. MMP inhibition significantly decreased migration of smooth muscle cells in pillars (Figure 9, A and B, and Supplemental Video S1), but did not affect migration in deep smooth muscle cell layers (Figure 9, C and D, and Supplemental Videos S2 and S3). Smooth muscle cells migrated faster in deep layers than in pillars (both with and without MMP inhibitor), possibly reflecting the difference in both matrix and cell composition between the layers. In summary, the combined *in vitro* and *in vivo* data suggest that MMP-dependent proteolysis of extracellular matrix proteins allows cells to move and form pillars.

Discussion

This study presents evidence of intussusceptive angiogenesis in human melanoma metastases. Intraluminal pillars, the hallmark of intussusceptive angiogenesis, were found

within blood vessels in human metastases and had similar structure, as shown in embryonic and pathologic angiogenesis.[10,11,20,35,36]

Tumor angiogenesis has been an intense area of research for many decades, but there is surprisingly limited knowledge on how new blood vessels are formed within human tumors. Sprouting is often assumed to be the dominating angiogenic mechanism, but new blood vessels could also form via intussusceptive angiogenesis.[37–41] Intussusceptive angiogenesis may be underestimated because intraluminal pillars are not detected by conventional microscopy. Previously, intravascular pillars in tumors have mainly been visualized in experimental models using advanced three-dimensional reconstructions of serial ultrathin sections or vascular cast techniques.[5,9,14,16,17,19,41] In the current study, pillars were demonstrated and quantified using a combination of more widely available epifluorescence and confocal microscopy. Using this approach, pillars were detected in high numbers in human melanoma metastases. More important, there are very few previous studies on intussusceptive angiogenesis in human tumors.[37–39] In one of these previous studies, phase contrast microscopy demonstrated intraluminal tissue folds, a histologic feature indicating intussusceptive angiogenesis, extending across the blood vessel lumen in primary melanomas.[38] Interestingly, intraluminal tissue folds were more commonly detected in thick than in thin primary melanomas. Thick melanomas are more aggressive and prone to metastasize, suggesting that intussusceptive angiogenesis may be linked to a more aggressive tumor biology.

Intussusceptive and sprouting angiogenesis are probably complementary, rather than independent, processes in tumor development and progression. Sprouting allows introduction of blood vessels into an avascular space.[20,42,43] Once the basic vascular network is formed by sprouting, an angioadaptive switch to intussusceptive angiogenesis occurs.[44] During intussusceptive angiogenesis, single vessels divide into two new vessels by the insertion and expansion of intraluminal pillars. In this way, the initial plexus expands and remodels into a larger vascular network.[35,42] In agreement with this hypothesis, pillars were predominantly detected in the peripheral zone, including the adjacent stroma, of human melanoma metastases, rather than in the more hypoxic tumor center. Similar peripheral localization of intussusceptive angiogenesis has been reported in a mouse model of colorectal cancer.[20] In addition, there was significantly lower endothelial cell proliferation in pillar zones compared with nonpillar zones. This observation supports that intussusceptive angiogenesis is present in pillar zones because intussusceptive blood vessels, in contrast to sprouting vessels, are mainly nonproliferative.[5,9]

A higher expression of MMP9 mRNA was detected in human pillar-rich metastases than in pillar-poor PDXs. More important, the presence of MMP9 protein adjacent to and inside of pillars was also verified. MMPs are master regulators of remodeling[45] and have previously been implicated in both intussusceptive and sprouting angiogenesis.[46,47] This led us to hypothesize that MMPs are important in pillar formation. MMP inhibition decreased pillar formation *in vitro*. In contrast, MMP inhibition had no effect on sprouting angiogenesis and vasculogenesis (*de novo* formation of blood vessels) *in vitro*. Furthermore, live-cell analysis showed that MMP inhibition reduced the migration of smooth muscle cells through established pillars. Accordingly, MMP inhibition may prevent the basement membrane remodeling and smooth muscle migration required for pillar formation. In addition to MMP9, mRNA levels of MMPs 2, 7, and 11 were expressed nominally higher in human tumors, but the difference was not significant. Data from genetically modified mice have established that knockout of a single MMP is often compensated by increased activity of other MMPs.[45] For example, knockout of MMP9 is compensated by increased MMP2 activity. Both MMP9 and MMP2 degrade basement membrane protein collagen IV and may thus be required for basement membrane remodeling during intussusceptive angiogenesis. As a further level of complexity, there is also cross talk between MMPs (eg, MMP14/membrane type-1 (MT-1), an important activator of MMP2). Because of such compensations and cross talk, broad-spectrum MMP inhibitors targeting many MMPs simultaneously are probably required to inhibit intussusceptive angiogenesis.

MMPs have recently been shown to have an additional role in intussusceptive angiogenesis that is not related to matrix remodeling. In a mouse-colitis model, endothelial cell MMP14/MT1-MMP cleaves thrombospondin-1 to generate C-terminal fragments of thrombospondin-1.[47] These fragments bind αvβ3 integrin and lead to nitric oxide production, which induces vasodilation in arterioles and thus initiates intussusceptive angiogenesis. This observation further supports the rationale to use MMP inhibitors to block intussusceptive angiogenesis. However, it will be essential to establish animal melanoma models to directly investigate if MMP inhibition blocks intussusceptive angiogenesis *in vivo*.

Both human and experimental evidence suggests that inflammation promotes intussusceptive angiogenesis.[13–15,17,47] The study found higher degrees of intussusceptive angiogenesis in human tumors, with more intratumoral inflammation, compared with mouse tumors with less inflammation. In human metastases, both macrophages and T cells were detected in higher numbers in close proximity to pillars compared with blood vessels without pillars. These results suggest that macrophages and T cells may promote pillar formation. These results are thus in line with previously published observations. However, the exact mechanism explaining how macrophages and T cells promote intussusceptive angiogenesis remains to be determined. One contributing factor may be MMP9 production by

macrophages, as macrophages often are a major source of MMP9 in tumors.[48]

There are several limitations to the study. Pillar quantification was performed on thin tissue sections, and only pillars with a confirmed three-dimensional structure verified with confocal microscopy were included. Pillars torn by sectioning and small endothelial pillars in blood vessels without smooth muscle cells, such as postcapillary venules, were not counted. Therefore, the technique used is likely to underestimate the true number of pillars. However, this would not influence the relative differences in pillars between human metastases and mouse tumors. Finally, the *in vitro* system used to study pillar formation has several limitations. The model lacks important components that are likely to initiate pillar formation *in vivo*, such as immune cells and blood flow. There is solid evidence indicating an important role of flow hemodynamics in intussusceptive angiogenesis.[5,9,14,35,40–44,48] In particular, flow-induced release of nitric oxide from endothelial cells seems to be essential for initiation of intussusception *in vivo*. In our model, pillars form spontaneously and in the absence of flow. Therefore, the *in vitro* model used herein is not suitable to define factors that initiate pillar formation. *In vivo* models would be needed to define those factors. The strength of our model is that it constitutes a flexible system to study the mechanics of pillar assembly, such as the matrix remodeling and cell movements described in this article.

In conclusion, the findings in this study suggest that intussusceptive angiogenesis may contribute to the growth of human melanoma metastases. Furthermore, MMP inhibition may be a new therapeutic strategy to inhibit intussusceptive angiogenesis. Combined targeting of intussusceptive angiogenesis and sprouting angiogenesis should be further explored as a treatment option in therapy-resistant metastatic melanomas.

Acknowledgment

We thank Kristina Skålén for technical assistance.

Supplemental Data

Supplemental material for this article can be found at *http://doi.org/10.1016/j.ajpath.2021.07.009*.

References

1. Folkman J: Tumor angiogenesis: therapeutic implications. N Engl J Med 1971, 285:1182–1186
2. Carmeliet P: Angiogenesis in life, disease and medicine. Nature 2005, 438:932–936
3. Ebos JM, Kerbel RS: Antiangiogenic therapy: impact on invasion, disease progression, and metastasis. Nat Rev Clin Oncol 2011, 8: 210–221
4. Bergers G, Hanahan D: Modes of resistance to anti-angiogenic therapy. Nat Rev Cancer 2008, 8:592–603
5. De Spiegelaere W, Casteleyn C, Van den Broeck W, Plendl J, Bahramsoltani M, Simoens P, Djonov V, Cornillie P: Intussusceptive angiogenesis: a biologically relevant form of angiogenesis. J Vasc Res 2012, 49:390–404
6. Ribatti D, Crivellato E: "Sprouting angiogenesis", a reappraisal. Dev Biol 2012, 372:157–165
7. Ausprunk DH, Folkman J: Migration and proliferation of endothelial cells in preformed and newly formed blood vessels during tumor angiogenesis. Microvasc Res 1977, 14:53–65
8. Gerhardt H, Golding M, Fruttiger M, Ruhrberg C, Lundkvist A, Abramsson A, Jeltsch M, Mitchell C, Alitalo K, Shima D, Betsholtz C: VEGF guides angiogenic sprouting utilizing endothelial tip cell filopodia. J Cell Biol 2003, 161:1163–1177
9. Burri PH, Djonov V: Intussusceptive angiogenesis–the alternative to capillary sprouting. Mol Aspects Med 2002, 23:S1–S27
10. Caduff JH, Fischer LC, Burri PH: Scanning electron microscope study of the developing microvasculature in the postnatal rat lung. Anat Rec 1986, 216:154–164
11. Burri PH, Tarek MR: A novel mechanism of capillary growth in the rat pulmonary microcirculation. Anat Rec 1990, 228:35–45
12. Kilarski WW, Gerwins P: A new mechanism of blood vessel growth - hope for new treatment strategies. Discov Med 2009, 8:23–27
13. Konerding MA, Turhan A, Ravnic DJ, Lin M, Fuchs C, Secomb TW, Tsuda A, Mentzer SJ: Inflammation-induced intussusceptive angiogenesis in murine colitis. Anat Rec (Hoboken) 2010, 293:849–857
14. Dimova I, Hlushchuk R, Makanya A, Styp-Rekowska B, Ceausu A, Flueckiger S, Lang S, Semela D, Le Noble F, Chatterjee S, Djonov V: Inhibition of Notch signaling induces extensive intussusceptive neoangiogenesis by recruitment of mononuclear cells. Angiogenesis 2013, 16:921–937
15. Ackermann M, Verleden SE, Kuehnel M, Haverich A, Welte T, Laenger F, Vanstapel A, Werlein C, Stark H, Tzankov A, Li WW, Li VW, Mentzer SJ, Jonigk D: Pulmonary vascular endothelialitis, thrombosis, and angiogenesis in Covid-19. N Engl J Med 2020, 383:120–128
16. Oliveira de Oliveira LB, Faccin Bampi V, Ferreira Gomes C, Braga da Silva JL, Encarnação Fiala Rechsteiner SM: Morphological characterization of sprouting and intussusceptive angiogenesis by SEM in oral squamous cell carcinoma. Scanning 2014, 36:293–300
17. Ackermann M, Morse BA, Delventhal V, Carvajal IM, Konerding MA: Anti-VEGFR2 and anti-IGF-1R-Adnectins inhibit Ewing's sarcoma A673-xenograft growth and normalize tumor vascular architecture. Angiogenesis 2012, 15:685–695
18. Bugyik E, Dezso K, Reiniger L, László V, Tóvári J, Tímár J, Nagy P, Klepetko W, Döme B, Paku S: Lack of angiogenesis in experimental brain metastases. J Neuropathol Exp Neurol 2011, 70:979–991
19. Hlushchuk R, Riesterer O, Baum O, Wood J, Gruber G, Pruschy M, Djonov V: Tumor recovery by angiogenic switch from sprouting to intussusceptive angiogenesis after treatment with PTK787/ZK222584 or ionizing radiation. Am J Pathol 2008, 173: 1173–1185
20. Paku S, Dezso K, Bugyik E, Tóvári J, Tímár J, Nagy P, Laszlo V, Klepetko W, Döme B: A new mechanism for pillar formation during tumor-induced intussusceptive angiogenesis: inverse sprouting. Am J Pathol 2011, 179:1573–1585
21. Felcht M, Thomas M: Angiogenesis in malignant melanoma. J Dtsch Dermatol Ges 2015, 13:125–136
22. Corrie PG, Basu B, Zaki KA: Targeting angiogenesis in melanoma: prospects for the future. Ther Adv Med Oncol 2010, 2: 367–380
23. Einarsdottir BO, Bagge RO, Bhadury J, Jespersen H, Mattsson J, Nilsson LM, Truvé K, López MD, Naredi P, Nilsson O, Stierner U, Ny L, Nilsson JA: Melanoma patient-derived xenografts accurately model the disease and develop fast enough to guide treatment decisions. Oncotarget 2014, 5:9609–9618

24. Dankort D, Curley DP, Cartlidge RA, Nelson B, Karnezis AN, Damsky WE Jr, You MJ, DePinho RA, McMahon M, Bosenberg M: Braf(V600E) cooperates with Pten loss to induce metastatic melanoma. Nat Genet 2009, 41:544−552
25. Le Gal K, Ibrahim MX, Wiel C, Sayin VI, Akula MK, Karlsson C, Dalin MG, Akyürek LM, Lindahl P, Nilsson J, Bergo MO: Antioxidants can increase melanoma metastasis in mice. Sci Transl Med 2015, 7:308re8
26. Kijani S, Yrlid U, Heyden M, Levin M, Borén J, Fogelstrand P: Filter-dense multicolor microscopy. PLoS One 2015, 10:e0119499
27. Einarsdottir BO, Karlsson J, Söderberg EMV, Lindberg MF, Funck-Brentano E, Jespersen H, Brynjolfsson SF, Olofsson Bagge R, Carstam L, Scobie M, Koolmeister T, Wallner O, Stierner U, Berglund UW, Ny L, Nilsson LM, Larsson E, Helleday T, Nilsson JA: A patient-derived xenograft pre-clinical trial reveals treatment responses and a resistance mechanism to karonudib in metastatic melanoma. Cell Death Dis 2018, 9:810
28. Ny L, Rizzo LY, Belgrano V, Karlsson J, Jespersen H, Carstam L, Bagge RO, Nilsson LM, Nilsson JA: Supporting clinical decision making in advanced melanoma by preclinical testing in personalized immune-humanized xenograft mouse models. Ann Oncol 2020, 31:266−273
29. Dobin A, Davis CA, Schlesinger F, Drenkow J, Zaleski C, Jha S, Batut P, Chaisson M, Gingeras TR: STAR: ultrafast universal RNA-seq aligner. Bioinformatics 2013, 29:15−21
30. Harrow J, Frankish A, Gonzalez JM, Tapanari E, Diekhans M, Kokocinski F, et al: GENCODE: the reference human genome annotation for the ENCODE Project. Genome Res 2012, 22:1760−1774
31. Ahdesmäki MJ, Gray SR, Johnson JH, Lai Z: Disambiguate: an open-source application for disambiguating two species in next generation sequencing data from grafted samples. F1000Res 2016, 5:2741
32. Anders S, Pyl PT, Huber W: HTSeq–a Python framework to work with high-throughput sequencing data. Bioinformatics 2015, 31:166−169
33. Levin M, Ewald AJ, McMahon M, Werb Z, Mostov K: A model of intussusceptive angiogenesis. Novartis Found Symp 2007, 283:37−42; discussion 42-45, 238-241
34. Love MI, Huber W, Anders S: Moderated estimation of fold change and dispersion for RNA-seq data with DESeq2. Genome Biol 2014, 15:550
35. Djonov V, Schmid M, Tschanz SA, Burri PH: Intussusceptive angiogenesis: its role in embryonic vascular network formation. Circ Res 2000, 86:286−292
36. Burri PH: Intussusceptive microvascular growth, a new mechanism of capillary network formation. EXS 1992, 61:32−39
37. Nico B, Crivellato E, Guidolin D, Annese T, Longo V, Finato N, Vacca A, Ribatti D: Intussusceptive microvascular growth in human glioma. Clin Exp Med 2010, 10:93−98
38. Ribatti D, Nico B, Floris C, Mangieri D, Piras F, Ennas MG, Vacca A, Sirigu P: Microvascular density, vascular endothelial growth factor immunoreactivity in tumor cells, vessel diameter and intussusceptive microvascular growth in primary melanoma. Oncol Rep 2005, 14:81−84
39. Zhang Z, Zhao M, Xu Z, Song Z: Angioarchitecture and CD133 + tumor stem cell distribution in intracranial hemangiopericytoma: a comparative study with meningioma. Neural Regen Res 2011, 6:2687−2693
40. Nowak-Sliwinska P, Alitalo K, Allen E, Anisimov A, Aplin AC, Auerbach R, et al: Consensus guidelines for the use and interpretation of angiogenesis assays. Angiogenesis 2018, 21:425−532
41. Burri PH, Hlushchuk R, Djonov V: Intussusceptive angiogenesis: its emergence, its characteristics, and its significance. Dev Dyn 2004, 231:474−488
42. Makanya AN, Stauffer D, Ribatti D, Burri PH, Djonov V: Microvascular growth, development, and remodeling in the embryonic avian kidney: the interplay between sprouting and intussusceptive angiogenic mechanisms. Microsc Res Tech 2005, 66:275−288
43. Makanya AN, Hlushchuk R, Djonov V: Intussusceptive angiogenesis and its role in vascular morphogenesis, patterning, and remodeling. Angiogenesis 2009, 12:113−123
44. Hlushchuk R, Makanya AN, Djonov V: Escape mechanisms after antiangiogenic treatment, or why are the tumors growing again? Int J Dev Biol 2011, 55:563−567
45. Bonnans C, Chou J, Werb Z: Remodelling the extracellular matrix in development and disease. Nat Rev Mol Cell Biol 2014, 15:786−801
46. Ackermann M, Stark H, Neubert L, Schubert S, Borchert P, Linz F, Wagner WL, Stiller W, Wielpütz M, Hoefer A, Haverich A, Mentzer SJ, Shah HR, Welte T, Kuehnel M, Jonigk M: Morpho-molecular motifs of pulmonary neoangiogenesis in interstitial lung diseases. Eur Respir J 2020, 55:1900933
47. Esteban S, Clemente C, Koziol A, Gonzalo P, Rius C, Martínez F, Linares PM, Chaparro M, Urzainqui A, AndrésV, Seiki M, Gisbert JP, Arroyoet AG: Endothelial MT1-MMP targeting limits intussusceptive angiogenesis and colitis via TSP1/nitric oxide axis. EMBO Mol Med 2020, 12:e10862
48. Riabov V, Gudima A, Wang N, Mickley A, Orekhov A, Kzhyshkowska J: Role of tumor associated macrophages in tumor angiogenesis and lymphangiogenesis. Front Physiol 2014, 5:1−13